Differential Modification of Phosducin Protein in Degenerating rd1 Retina Is Associated with Constitutively Active Ca^{2+}/Calmodulin Kinase II in Rod Outer Segments*

Stefanie M. Hauck‡§, Per A. R. Ekström§¶‖, Poonam Ahuja-Jensen¶, Sabine Suppmann‡, Francois Paquet-Durand¶, Theo van Veen¶, and Marius Ueffing‡

Retinitis pigmentosa comprises a heterogeneous group of incurable progressive blinding diseases with unknown pathogenic mechanisms. The retinal degeneration 1 (rd1) mouse is a retinitis pigmentosa model that carries a mutation in a rod photoreceptor-specific phosphodiesterase gene, leading to rapid degeneration of these cells. Elucidation of the molecular differences between rd1 and healthy retinae is crucial for explaining this degeneration and could assist in suggesting novel therapies. Here we used high resolution proteomics to compare the proteomes of the rd1 mouse retina and its congenic, wild-type counterpart at postnatal day 11 when photoreceptor death is profound. Over 3000 protein spots were consistently resolved by two-dimensional gel electrophoresis and subjected to a rigorous filtering procedure involving computer-based spot analyses. Five proteins were accepted as being differentially expressed in the rd1 model and subsequently identified by mass spectrometry. The difference in one such protein, phosducin, related to an altered modification pattern in the rd1 retina rather than to changed expression levels. Additional experiments showed phosducin in healthy retinae to be highly phosphorylated in the dark- but not in the light-adapted phase. In contrast, rd1 phosducin was highly phosphorylated irrespective of light status, indicating a dysfunctional rd1 light/dark response. The increased rd1 phosducin phosphorylation coincided with increased activation of calcium/calmodulin-activated protein kinase II, which is known to utilize phosducin as a substrate. Given the increased rod calcium levels present in the rd1 mutation, calcium-evoked overactivation of this kinase may be an early and long sought for step in events leading to photoreceptor degeneration in the rd1 mouse. ***Molecular & Cellular Proteomics 5:324–336, 2006.***

Photoreceptor degeneration resulting from genetic mutation or age is a major cause of progressive vision loss in the western world. Therapeutic prevention of this process, however, is hindered as the molecular pathomechanisms of degeneration are currently not well defined. To aid in their elucidation, several animal models for photoreceptor degeneration exist, including the retinal degeneration 1 (rd1)[1] mouse, which carries a non-sense mutation in the gene coding for the β subunit of the rod photoreceptor-specific cGMP phosphodiesterase 6 (PDE6-β) (1, 2). Because mutations of the same gene have been linked to some forms of the human disease retinitis pigmentosa (3), the rd1 model is a relevant tool for studying various aspects of human retinal degeneration.

As a consequence of the rd1 mutation, PDE6-β expression in rods yields a nonfunctional protein leading to cGMP accumulation in the cytoplasm of rod outer segments (4). Normal regulation of rod cGMP-gated cation channels occurs through cGMP fluctuations generated by the phototransduction cascade (5, 6), and the cGMP accumulation found in rd1 rods is therefore a likely cause for the abnormally high Ca^{2+} levels detected in the rd1 retina (7, 8). Increased intracellular Ca^{2+} *per se* has been correlated with rod cell death (8, 9), and it is reasonable that uncontrolled Ca^{2+} influx into rd1 rods triggers apoptosis, which characterizes the photoreceptor degeneration in this model (10–12). In accordance, Ca^{2+} channel blockers have been shown to rescue rd1 photoreceptors (13, 14). However, although a consensus on the role of Ca^{2+} as initiator of degeneration in the rd1 retina may exist, the cellular

From the ‡GSF-National Research Centre for Environment and Health, Institute of Human Genetics, Neuherberg 85764, Germany and the ¶Department of Ophthalmology, Lund University, BMC-B13, SE-221 84 Lund, Sweden

Received, July 15, 2005, and in revised form, October 20, 2005
Published, MCP Papers in Press, October 26, 2005, 10.1074/mcp.M500217-MCP200

[1] The abbreviations used are: rd1, retinal degeneration 1; 2DE, two-dimensional electrophoresis; CaBP, Ca^{2+}-binding protein; CaM, calmodulin; CaMKII, Ca^{2+}/calmodulin kinase II; pCaMKII, phospho-Ca^{2+}/calmodulin kinase II; Csn8, COP9 subunit 8; GC, guanylate cyclase; GCAP, guanylate cyclase-activating protein; GCL, ganglion cell layer; GK, guanylate kinase; GPCR, G protein-coupled receptor; GRK-2, G protein-coupled receptor kinase-2; HE, hematoxylin-eosin; INL, inner nuclear layer; IPL, inner plexiform layer; ONL, outer nuclear layer; PDE, phosphodiesterase; PFA, paraformaldehyde; PKA, protein kinase A; PN, postnatal day; PNA, peanut agglutinin; TUNEL, terminal deoxynucleotidyltransferase-mediated dUTP nick end labeling; WT, wild-type.

steps subsequent to this remain unresolved, leading for instance to conflicting views on whether caspase cascades underlie the execution of apoptosis. Whereas some studies have demonstrated caspase activation in rd1 retinae from the 2nd to 3rd postnatal week, *i.e.* at peak or postpeak of photoreceptor cell apoptosis (15–17), Doonan *et al.* (18) were unable to detect increased caspase expression or activation at these and earlier time points in the same tissue, and caspase inhibition or ablation of caspase-3 failed to rescue rd1 photoreceptors from apoptosis (19, 20). It has also been shown that rd1 photoreceptors degenerate irrespective of the expression of p53, a tumor suppressor gene involved in several types of apoptosis (21), or c-Fos (22), which by contrast is entirely essential for light-induced photoreceptor degeneration (23). With respect to antiapoptotic components, only minimal improvement of rd1 photoreceptor survival is observed by overexpressing survival-promoting genes, such as *bcl-2* (24), which prevents degeneration in other neuronal systems (25). Similarly we have observed an overactivation of the antiapoptotic Akt-kinase pathway in rd1 rods (26), but these cells degenerate nevertheless.

The unresolved issues and conflicting views on rd1 photoreceptor degeneration illustrate the necessity for clarifying the critical differences between the rd1 mutation and its congenic, wild-type (WT) counterpart. Such differences have been described at the transcriptome level using microarray techniques covering from ~600 to 12,000 genes and expression sequence tags (27–29). However, alterations in mRNA expression are not necessarily reflected in the altered expression of corresponding proteins or vice versa. It is therefore of interest that potential degeneration-related differences at the protein level between rd1 and WT retinae have been addressed recently by Cavusoglu *et al.* (30). Their study resolved ~250 protein spots by two-dimensional electrophoresis (2DE) and identified these by mass spectrometry, revealing differential levels of crystallin at a late developmental stage when degeneration of photoreceptors is complete. This underscores the potential of proteomic techniques to disclose protein alterations consequent to degeneration. It is likely, therefore, that by increasing the resolving power of the proteomic approach applied at earlier stages of degeneration the detection of subtler differences directly related to or even preceding the death process should be possible.

In the present study we used a high resolution 2DE system consistently able to resolve ~3000 protein spots. The separations were coupled with computer-assisted gel analysis to select differentially regulated protein spots for subsequent identification by mass spectrometry. Postnatal day 11 (PN11) was selected as the time point for rd1/WT comparisons because the number of photoreceptor cells is then still stable. Together with the use of whole retina samples, PN11 analysis reduces the risk of false positive protein differences related to the biased contribution of a particular cell type (photoreceptors) rather than to disease-associated changes. Relevant comparisons are therefore possible because active mechanisms committing cells to die are intense at PN11 (see *e.g.* Ref. 18). With this paradigm we identified previously unreported changes in the proteome of the young rd1 retina, including a differential post-translational modification of phosducin.

EXPERIMENTAL PROCEDURES

Animals and Tissue Preparation—All animal experiments were approved by the Swedish ethics committee (permits M9-02 and M213-03). Normal (C3H+/+, hereafter referred to as WT) and rd1 mutant (C3H *rd1/rd1*) mice were obtained from in-house breeding colonies. Mice (PN11) were sacrificed by asphyxiation on dry ice. For 2DE analyses, eyes were generally collected from light-adapted animals. For a subset of analyses and immunostaining studies, eyes were collected both from light- and dark-adapted mice. For these studies, animals from one litter were divided into two equal groups; one group was light-adapted, and the other was dark-adapted for a period of 6 h prior to enucleation of the eyes. Dark-adapted eyes were enucleated under red light and processed in the dark. For immunostaining studies, the eyes were removed and immediately immersed in 4% paraformaldehyde (PFA) in PBS on ice for 4 h and then transferred to 20% sucrose in Sörensen's phosphate buffer. After embedding, sections (cryostat; 8 μm) were collected on chrome alum-gelatinated slides (slides briefly dipped in warm solutions of 0.5% gelatin (Sigma) and 0.05% potassium chrome(III)-sulfate (Merck) in H_2O and allowed to dry at 60 °C prior to use). Tissue sections were stored at −20 °C until used for immunostaining.

Sample Preparation—For preparation of 2DE samples, dissected eyes were immediately immersed in ice-cold dissection buffer (10 mM Tris, 1 mM EDTA, 150 mM NaCl, 1 mM freshly activated Na_3VO_4, 50 nM okadaic acid, Complete protease inhibitor mixture, pH 7.5 with HCl). Retinae were dissected on ice and stored at −80 °C until use.

For each experiment, fresh WT and rd1 samples were prepared as follows. Fourteen retinae were pooled and homogenized with a Teflon glass homogenizer (Braun Biotech International) in 2 ml of ice-cold nanopure water containing a protease inhibitor mixture (Roche Applied Science). The homogenate was lyophilized and stored at −80 °C. Prior to 2DE, proteins were solubilized in denaturing lysis buffer (9 M urea, 2 M thiourea, 4% CHAPS, 1% dithioerythritol, 2.5 mM EDTA, and 2.5 mM EGTA) for 4 h at room temperature. Samples were cleared by centrifugation (50,000 × *g* for 50 min), and protein concentrations were determined by Bradford assay (Bio-Rad). Protein resolution was done by loading 150 and 500 μg of total proteins from each sample onto analytical and preparative two-dimensional gels, respectively

Preparation of 2DE samples from dark- and light-adapted eyes involved enucleation, immediate freezing, and storage at −80 °C until further use. The complete eyes were then homogenized and processed as described above.

2DE—First dimension isoelectric focusing was performed using either 11- or 24-cm, pH 3–10 or 4–7 linear gradient IPG strips (Amersham Biosciences). Strips were rehydrated overnight with the samples additionally containing 0.7% (v/v) Pharmalytes™ 3–10 (Amersham Biosciences) and 0.25% (w/v) bromphenol blue. Isoelectric focusing and second dimension PAGE were carried out as described by Hauck *et al.* (31). Gels used for image analysis were silver-stained (32) and dried between cellophane sheets.

Image Analysis—An experiment comprised six gels each from WT and rd1 retinae processed in parallel. In each experiment, three to four gels from either condition were selected for quality of focusing and scanned on a transmission scanner (Epson GT-9600) with 12

bit/300 dpi resolution, and resultant gel images were then imported to a 2DE analysis software program (Proteom Weaver, release 2.1.; Definiens, Germany). The following parameters for protein spot detection were used: minimum spot radius of 4, minimum spot intensity (volume above base level) of 2000, and minimum contrast (height above base level) of 10. Gels from each experiment were processed by the pair-match-based normalization, which erases intensity differences of similar spots in different gels not due to regulation but experimental variability of the method (*e.g.* protein load or silver stain intensity). Subsequently respective WT and rd1 protein spots were matched and filtered to find significant differences within the detection limit as follows. Only spots matched in at least two-thirds of the gel images were considered, and only these filtered spots exceeding an intensity threshold of 0.1 were taken for further analysis. The remaining spots were sorted according to a regulation factor (quotient of rd1 and WT intensities), and for each experimental set, the threshold regulation factor for the significance level $p < 0.05$ was determined by the Proteom Weaver software. Only those spots regulated more than the factor required for significance were further considered as candidate spots and subsequently subjected to manual verification for matching accuracy to avoid assigning false positives. The entire experiment was performed in triplicate.

In-gel Proteolysis and Identification by Mass Spectrometry—Regulated spots identified by image analysis were selected for identification and either excised from experimental 2DE gels (150-μg protein load) or the respective spots were excised from preparative gels (500-μg protein load). Spots were washed for 30 min in 100 μl of nanopure water, destained (33), and dehydrated in 100 μl of 40% acetonitrile (3 $\times$ 15 min). Samples were subjected to tryptic proteolysis in 5–10 μl of 1 mM Tris-HCl, pH 7.5, containing 0.01 μg/μl trypsin (sequencing grade modified trypsin, Promega) overnight at 37 °C.

MALDI-TOF peptide mass fingerprints were obtained on a Bruker Reflex III mass spectrometer (Bruker Daltonics, Bremen, Germany) as described previously (31). Peptide sequence information was obtained by LC-coupled MS/MS analysis on a Q-TOF2 system (Micromass) coupled with a CapLC system (Micromass) as described previously (31).

Database Searching—Database searches were performed using the Mascot software (34) at the following parameter settings: one miscleavage allowed, search restricted to database entries from metazoa; MALDI-TOF, 100 ppm mass accuracy; Q-TOF, 0.8-Da peptide tolerances; 0.2-Da MS/MS tolerance. Peptide masses of the tryptic digests were compared with the virtually generated tryptic peptide masses of the National Center for Biotechnology Information non-redundant (NCBInr) protein database and the Mass Spectrometry Protein Sequence Database (MSDB).

Western Blotting—Protein patterns from small 2DE gels comprising all experimental conditions (WT, dark and light; rd1, dark and light) were blotted semidry onto one PVDF membrane. Unspecific binding was blocked with 5% BSA in TBS-T (50 mM Tris, pH 7.4, 150 mM NaCl, 2 mM EDTA, and 0.1% Tween 20) for 1 h and incubated in primary antibody (rabbit anti-phosducin, 1:1000, a kind gift from M. Castro, University of Würzburg, Würzburg, Germany) at 4 °C overnight and then followed by the horseradish peroxidase-coupled secondary antibody (anti-rabbit IgG, Jackson Laboratories, 1:15,000). Signal was developed by ECL+ kit (Amersham Biosciences) according to the manufacturer's instructions and detected on Hyperfilm (Amersham Biosciences).

Immunofluorescence—Cryosections (8 μm) of 4% PFA-fixed WT or rd1 retinae were blocked in 10% goat serum in buffer (PBS with 0.25% Triton X-100 and 1% bovine serum albumin) and incubated overnight at 4 °C in one of the following primary antibodies: phosducin (1:500), Thr-286 phospho-Ca^{2+}/calmodulin kinase II (pCaMKII, Cell Signaling Technology, catalog number 3361; 1:400), Thr-286 pCaMKII (Promega, V1111; 1:200), total Ca^{2+}/calmodulin kinase II (CaMKII) (Cell Signaling Technology, catalog number 3362; 1:100), or calmodulin (CaM, Chemicon, catalog number MAB1040; 1:200). Cones were labeled with rhodamine-coupled peanut agglutinin (PNA, Vector Laboratories, catalog number FL1071; 1:800). Control experiments involved omission of primary antibodies or replacement with purified immunoglobulin G (Chemicon International; mouse, catalog number PP54; rabbit, catalog number PP64) at concentrations identical to those of the primary antibodies. After incubation, sections were washed and incubated with the appropriate fluorescent goat secondary antibodies (Alexa-coupled, Molecular Probes, 1:250) for 1 h at room temperature. After washing and mounting with Glycergel (Dako), the sections were examined and photographed with either a Zeiss Axiophot photomicroscope with Axiovision 4.1 software or a Nikon E800 equipped with an Olympus DP70 digital camera and AnalySIS 3.2 software. Confocal images were taken with a Leica TCS SP2 laser confocal microscope.

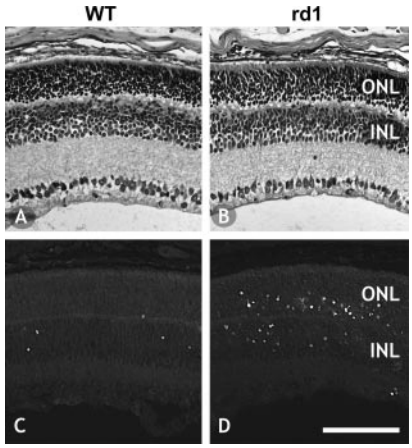

FIG. 1. **Histological analysis of WT (*A* and *C*) and rd1 retinae (*B* and *D*) at PN11.** HE-stained sections of murine PN11 retinae (*A* and *B*) revealed identical tissue morphology between WT (*A*) and rd1 (*B*) genotypes. TUNEL staining, however, demonstrated the presence of apoptotic cells in the ONL of rd1 retina (*D*) in contrast to WT retina (*C*). Residual developmental apoptosis of cells in the INL could be seen in both genotypes. *Scale bar*, 100 μm.

Terminal Deoxynucleotidyltransferase-mediated dUTP Nick End Labeling (TUNEL) Staining—Sections as above were washed 4 $\times$ 5 min in PBS and incubated with 10% goat serum. TUNEL staining for apoptotic nuclei was done using an *in situ* cell death detection kit (Roche Diagnostics) conjugated with FITC.

Hematoxylin-Eosin Staining—For general light microscopic analysis, tissue sections of paraffin-embedded, PFA-fixed retinae were stained with hematoxylin-eosin (HE) according to standard protocols.

RESULTS

Retinal Morphology Is Unaltered in rd1 Retina at PN11, but Photoreceptor Apoptosis Is Abundant—The rd1 mutation presents with a very early and rapid photoreceptor degeneration (10–12). To define the postnatal time point at which disease-induced apoptosis is most abundant while tissue morphology is still unaltered, sections from rd1 and WT retinae at PN7–13 were stained with HE and TUNEL. We found that although PN11 represents a developmental stage involving abundant photoreceptor apoptosis in the rd1 outer nuclear layer (ONL)

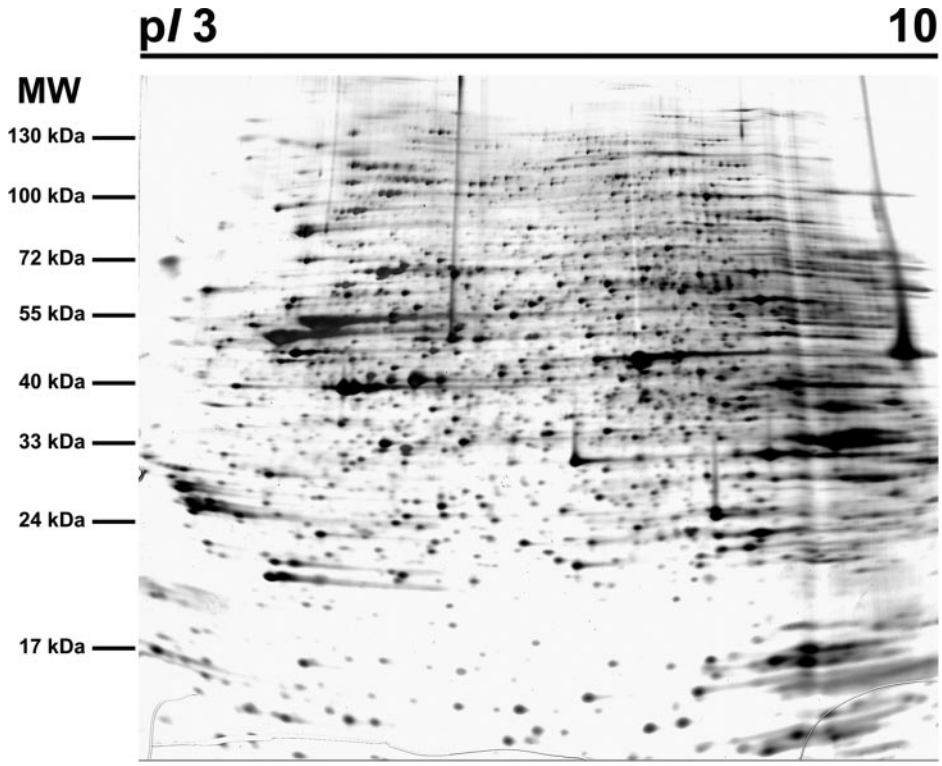

FIG. 2. **2DE analysis of retinal extract at PN11.** Shown is a representative 2DE gel of whole murine rd1 retina in which 150 μg of protein sample was resolved as described under "Experimental Procedures." Approximately 3300 protein spots were consistently detected on silver-stained gel images. Molecular masses of standards and pI are indicated.

(Fig. 1, *C* and *D*), the cellular integrity and thickness of this structure was comparable to WT (Fig. 1, *A* and *B*). Thus PN11 offers the advantage of reduced bias risk in comparisons of protein expression patterns. Conversely the high incidence of disease-related apoptosis provides an opportunity to detect differential expression of important proteins. Consequently PN11 retinae from rd1 and WT mice were subjected to 2DE-based comparisons to identify proteins potentially involved in early processes of retinal degeneration.

Differentially Expressed Proteins at PN 11: 2DE Analysis of Wild-type Versus rd1 Retina—An average of 3348 $\pm$ 352 protein spots were detected on each gel separation. One typical 2DE separation is shown in Fig. 2. Statistically significant changes within one experiment were filtered with the 2DE analysis software as described in detail under "Experimental Procedures." To eliminate false positive candidates, experimental variability was controlled on several levels as follows. (*a*) All gels from one experiment were processed in parallel. (*b*) Gel-to-gel variations due to experimental procedure were eliminated by pair-match-based normalization mode using an algorithm in the 2DE image analysis software. (*c*) The statistically significant regulation factor threshold was determined separately for each experimental set of 2DE gels ($p < 0.05$). (*d*) rd1 and WT retina comparisons at PN11 were performed in triplicate.

Because of this high stringency, only five of all possible detected proteins remained as candidates for differential expression in rd1 to WT comparisons (Fig. 3 and Table I). Two proteins in the rd1 retina, COP9 subunit 8 and 14-3-3 ζ, were up-regulated by 2.6 and 1.9-fold, respectively, as compared with WT. Conversely two proteins, β-adaptin and guanylate kinase, were down-regulated by 0.4 and 0.5-fold, respectively. The fifth candidate protein, phosducin, was found to be both up- and down-regulated in rd1 retina. Phosducin resolved on the 2DE gels as a group of spots (labeled 1–7 in Fig. 4*A*), along the acidic-to-basic axis (approximate pI, 4.32–4.60), with a concomitant but limited alteration in apparent molecular weight. According to mass spectrometric identifications, five of these spots (spots 2–6) contained the same protein, phosducin (Table I), suggesting post-translational modifications of the protein. The remaining two spots (spots 1 and 7) were identified by immunoblotting with a phosducin-specific antibody (see below). In the rd1 condition, an up-regulation of the acidic isoforms was found together with a down-regulation of the basic isoforms ($\sim$50% reduction; see regulation factor list, Fig. 4*A*). Total retinal phosducin for rd1 and WT on 2DE gels was compared by obtaining the cumulative average intensities for all phosducin spots. No significant difference in total phosducin was found between rd1 and WT (Fig. 4*B*), indicating that detected differences were indeed related to basic-to-acidic shifts of the molecule instead of alterations in expression levels. This was further supported by phosducin immunofluorescence of WT and rd1 where no immediate differences in staining patterns could be detected (see Fig. 5, *A* and *B*) as well as on one-dimensional Western blot experiments (data not shown).

The rd1 phenotype is caused by a mutation at the PDE6-β subunit resulting in a significant decrease of both mRNA level

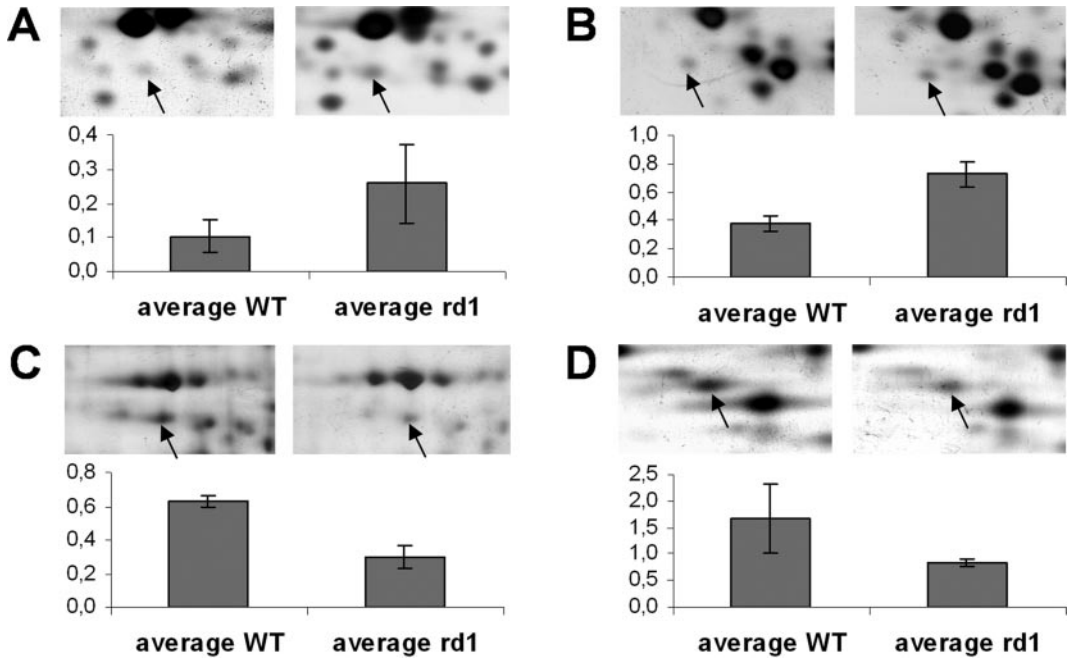

FIG. 3. **Differential protein expression in the rd1 retina.** 2DE-resolved proteins from WT and rd1 samples were detected and compared using an image analysis software as described under "Experimental Procedures." Experiments were performed in triplicate. Differential protein expression found in rd1 is shown: up-regulation of COP9 subunit 8 (*A*) and 14-3-3 ζ (*B*); down-regulation of β-adaptin (*C*) and guanylate kinase (*D*). *Shaded bars* represent absolute intensities (arbitrary units) quantified with image analysis software, and mean values derived from separate, triplicate experiments are given (*error bars* show SED). The photographic *insets above* each histogram show the appearance of the respective protein spots, indicated by *arrows*.

TABLE I
Mass spectrometric identifications of regulated proteins

Protein identity	Accession number	Mode of regulation	Score	Molecular weight	pI	
					Theoretical[a]	Observed
COP9 subunit 8 (CSN8_MOUSE)	Q8R4D2	Up-regulated in rd1	77	23,258	5.09	5.12
14-3-3 ζ (1433Z_MOUSE)	P63101	Up-regulated in rd1	82	27,925	4.73	4.59
β-Adaptin (AP2B1_MOUSE)	Q9DBG3	Down-regulated in rd1	104	105,428	5.22	5.31
Guanylate kinase (KGUA_MOUSE)	Q64520	Down-regulated in rd1	101	21,887	6.14	6.37
Phosducin spot 2 (PHOS_MOUSE)	Q9QW08	Up-regulated in rd1	142	28,016	4.45	4.40
Phosducin spot 3 (PHOS_MOUSE)	Q9QW08	Up-regulated in rd1	70	28,016	4.48	4.45
Phosducin spot 4 (PHOS_MOUSE)	Q9QW08	Up-regulated in rd1	153	28,016	4.52	4.50
Phosducin spot 5 (PHOS_MOUSE)	Q9QW08	Down-regulated in rd1	128	28,016	4.56	4.55
Phosducin spot 6 (PHOS_MOUSE)	Q9QW08	Down-regulated in rd1	175	28,016	4.59	4.60

[a] Calculated with compute pI/molecular weight program (ca.expasy.org/ or scansite.mit.edu/calc_mw_pi.html).

and PDE6-β activity (35, 36). We would therefore expect differential levels in PDE6-β protein expression between rd1 and WT. Indeed PDE6-β protein levels were high on one-dimensional Western blots of WT retina lysates but below detection levels in rd1 samples (data not shown). However, the protein could not be detected on 2DE blots of either rd1 or WT retina (not shown); this likely explains why PDE6-β failed to appear among the significantly regulated spots. This corroborates our previous experimental observations[2] in which PDE was excluded from 2DE gels but could be unequivocally detected by two-dimensional electrophoresis with cationic detergent benzyldimethyl-*n*-hexadecylammonium chloride (16-BAC) in the first dimension and SDS-PAGE in the second dimension, which allow separation and visualization of photoreceptor membrane and membrane-associated proteins.

Differential Modification of Phosducin Is Related to Impaired Light-Dark Adaptation—The separation of phosducin along the acidic-to-basic axis suggested post-translational modifications resulting in several pI isoforms of the molecule. The interspot pI distances observed (~0.05 pI units) are compatible with differential phosphorylation states of the phosducin protein as determined by the Scansite Molecular Weight and Isoelectric Point Calculator program (scansite.mit.edu/calc_mw_pi.html). Here

[2] S. Suppmann, J. Schoch, M. Swiatek-de Lange, S. M. Hauck, H. Zischka, and M. Ueffing, manuscript submitted.

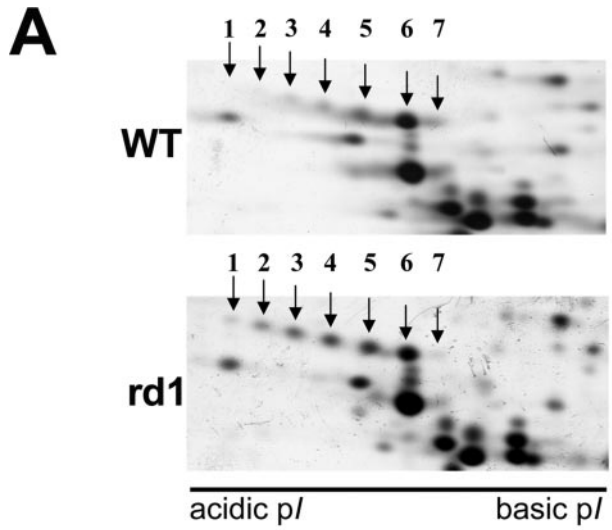

spot number	regulation factor in rd1 mice
1	below detection level in WT
2	2.03
3	1.95
4	1.71
5	0.85
6	0.53
7	0.48

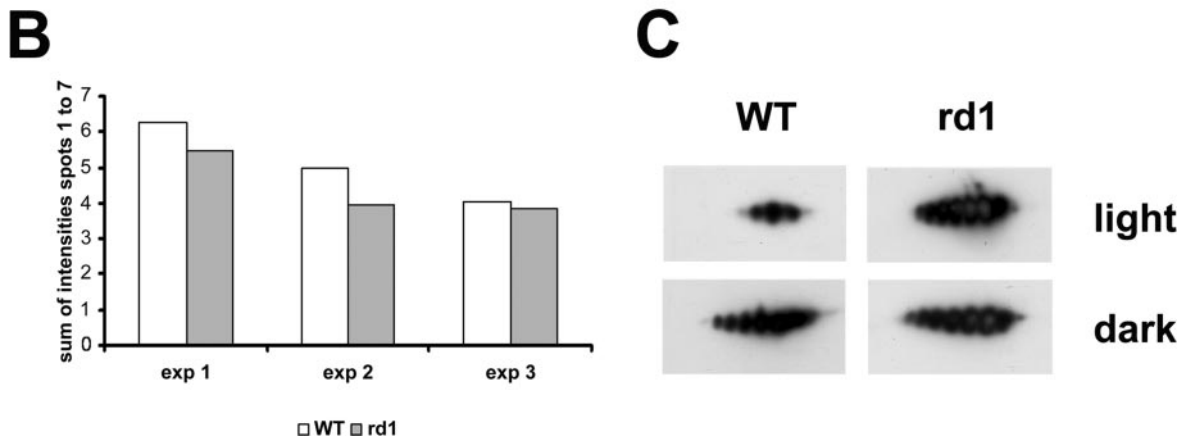

FIG. 4. **Analysis of differentially modified phosducin.** *A*, phosducin resolved on 2DE gels as a row of distinct spots (*1*–*7*, acidic to basic, respectively). The more acidic isoforms (1, 2, 3, and 4) were consistently up-regulated in the rd1 genotype. The most acidic phosducin isoform (equivalent to spot 1) was below the detection limit of silver stain in WT. The basic isoforms of phosducin (5, 6, and 7) were down-regulated in rd1 (mean regulation factor from three independent experiments is indicated). *B*, absolute intensities from spots 1–7 were added (WT, *open bars*; rd1, *filled bars*) within different experiments, and the cumulative phosducin intensity was compared between WT and rd1. No differences were found in phosducin levels between the genotypes. *C*, total eye extracts from light-adapted and dark-adapted WT and rd1 mice were resolved by 2DE, blotted, and probed with anti-phosducin antibody. WT dark-adapted eyes and rd1 dark- and light-adapted eyes showed similar phosducin spot separation patterns with seven different isoforms. In contrast, WT light-adapted eyes showed a phosducin separation pattern having only three isoforms. Blot image overlay revealed that these WT isoforms were the basic-most phosducin spots.

each added phosphate molecule leads to an increment in acidity of 0.04 pI units. The phosducin isoforms observed for rd1 retina were shifted toward the acidic side, which would be compatible with increased phosducin phosphorylation in the mutated state. Because phosducin is a well known retinal phosphoprotein whose increased phosphorylation has been linked to dim light adaptation in healthy phenotypes (37, 38), the question arose whether differences between rd1 and WT phosducin phosphorylation were related to light status. Hence WT and rd1 eyes at PN11 sampled during the light phase were compared with eyes collected in prolonged dark phase. Protein samples were resolved on 2DE gels, blotted, and probed for phosducin. Fig. 4*C* shows that immunoreactions could be separated into two categories. The full set of isoforms, including the acidic hyperphosphorylated forms of phosducin, was observed for WT only during the dark phase, whereas during the light phase WT displayed a clear reduction in the number of phosducin spots (*lower* and *upper left panel*, respectively), indicating reduced phosphorylation under light exposure. The rd1 retina, however, showed acidic, hyperphosphorylated forms of phosducin in both light and dark phases. When compared with WT retina, the phosphorylation states of rd1 phosducin in both light and dark phases were identical to the WT hyperphosphorylation state in darkness.

Differential Phosducin Phosphorylation Is Correlated with Differential Phosphorylation of CaMKII—Because of the differences in phosducin phosphorylation between rd1 and WT at the light-adapted state, we hypothesized that a kinase

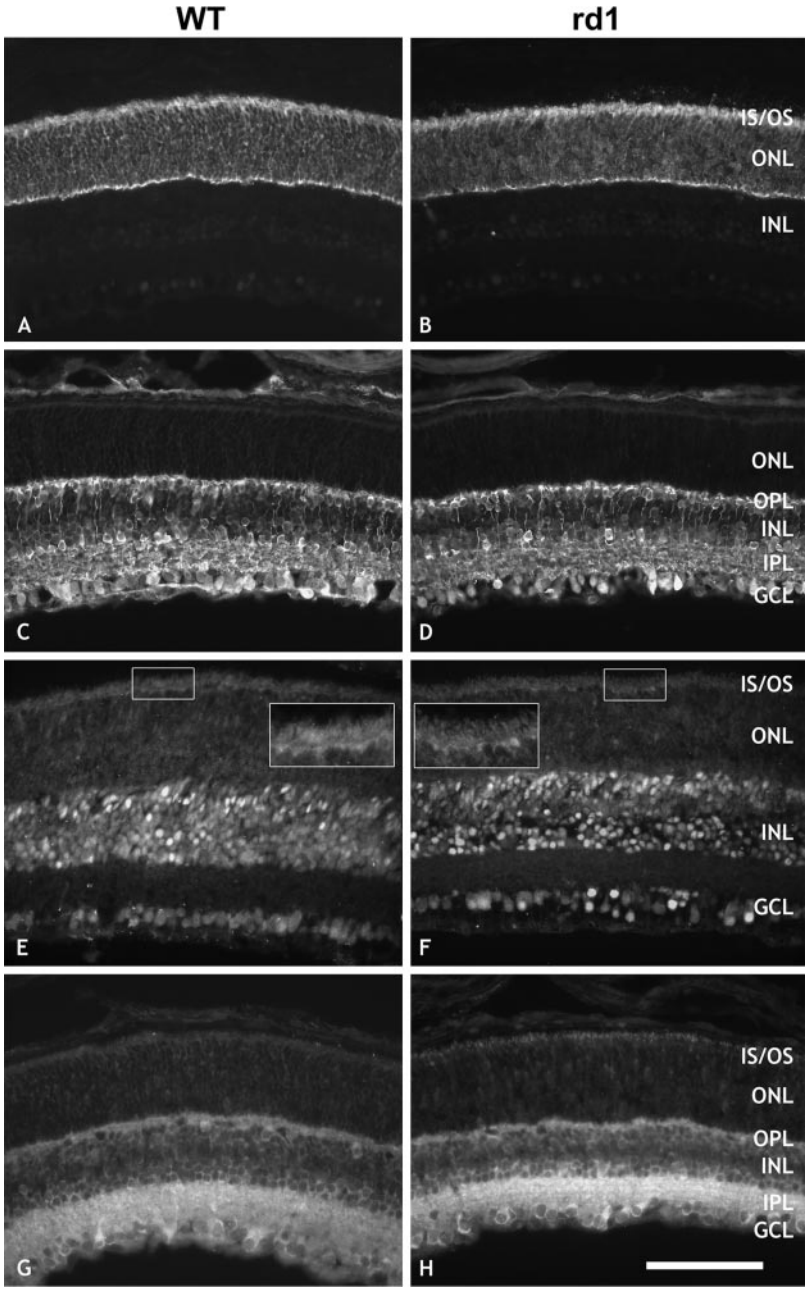

FIG. 5. **Immunofluorescent stainings of WT (*A*, *C*, *E*, and *G*) and rd1 (*B*, *D*, *F*, and *H*) retina on PN11.** Murine PN11 retina sections were stained with either anti-phosducin antibody (*A* and *B*), anti-calmodulin antibody (*C* and *D*), anti-total CaMKII antibody (*E* and *F*), or anti-pCaMKII antibody (*G* and *H*). Phosducin (*A* and *B*) was expressed exclusively in the photoreceptor layer. No differences were found between WT and rd1 in agreement with the unchanged total expression of total phosducin obtained by 2DE. Both calmodulin (*C* and *D*) and CaMKII (*E* and *F*) were expressed predominantly in inner retinal layers. CaMKII staining was also seen in the outer retina, including in the photoreceptor segment portion (see magnified *insets* in *E* and *F*). For both CaM and CaMKII no differences between WT and rd1 retinae could be detected. Similarly no staining differences between WT and rd1 were seen for pCaMKII at the inner retina (*G* and *H*). However, many more photoreceptor segments showed clear immunostaining for the phosphorylated protein in rd1 (*H*) compared with WT retinae (*G*). See Fig. 6 for further depiction of this phenomenon. *OPL*, outer plexiform layer; *IS/OS*, inner and outer segments of photoreceptors. *Large boxed insets* represent magnifications of selected areas of the photoreceptor segments indicated by the *smaller boxes*. *Scale bar* is 100 μm except for the magnified *insets* in *E* and *F* where it equals 50 μm.

responsible for the differential phosphorylation of phosducin may be differentially activated. Three distinct kinases are known to phosphorylate phosducin. Protein kinase A (PKA) and G protein-coupled receptor kinase-2 (GRK-2) have both been shown to contribute to phosducin modification on one phosphorylation site each (39, 40). In contrast, CaMKII was able to phosphorylate on five separate amino acids (Ser-6, Ser-36, Ser-54, Ser-73, and Ser-106) during *in vitro* experiments (41). Because we detected seven phosducin isoforms in the 2DE experiments that were all different between rd1 and WT (Fig. 4*A*), CaMKII is a likely candidate for contributing to the observed modification. Although CaMKII may not phosphorylate phosducin at more than the Ser-54 site, when analyzed under *in vivo* conditions (42), the phosphorylation of this site is particularly important for the interactions between phosducin and other retinal proteins, notably the 14-3-3 group of proteins (of which 14-3-3 ζ was found to be up-regulated here) and the photoreceptor-specific G-protein transducin (37, 38, 41–43). In light of this we immunostained retinal sections to assess the presence of possible differential CaMKII expression and/or activation in rd1 and WT.

Because CaMKII is dependent on Ca^{2+} and CaM for activation (44), we stained rd1 and WT PN11 retinae for CaM. Similar staining patterns were found for both genotypes (Fig.

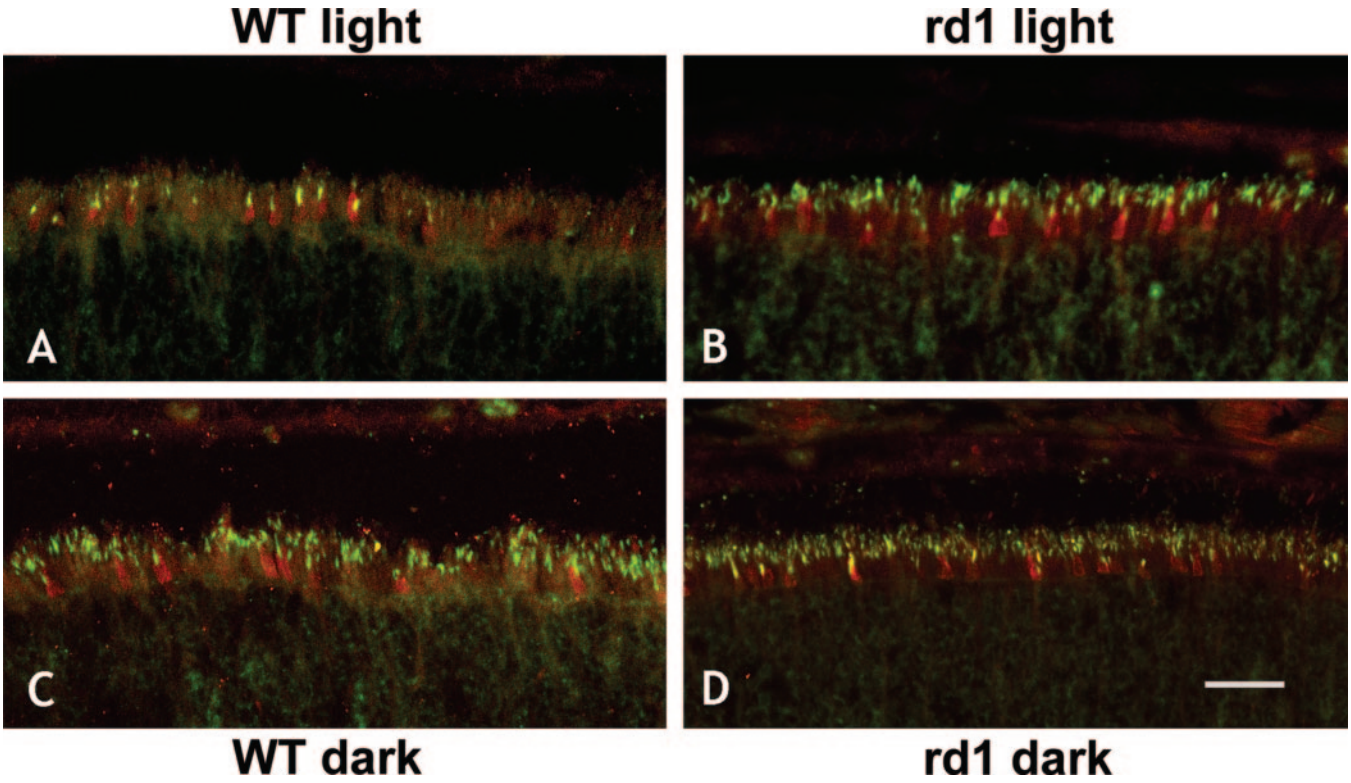

FIG. 6. **Confocal images of immunofluorescence detection of phosphorylated CaMKII (*green*) and PNA labeling (*red*).** Light-adapted (*A* and *B*) and dark-adapted (*C* and *D*) retinae from WT (*A* and *C*) and rd1 (*B* and *D*) at PN11 were stained with antibody against pCaMKII (*green* fluorescence) and labeled with fluorophore-coupled PNA to reveal the position of cone outer segments (*red* fluorescence). In the WT light-adapted phase, pCaMKII labeling was restricted to PNA-positive structures (*A*), whereas in all other cases pCaMKII was clearly also located in photoreceptor segments between the PNA-labeled structures, *i. e.* rod segments (*B*, *C*, and *D*). The differential staining between rd1 and WT in the light-adapted phase was seen in all examined retinae (at least five independent animals of each genotype) as were the similarities in the dark-adapted state (four eyes from two independent animals of each genotype). The retinal pigment epithelium is located at the *superior* aspect of each *panel*. *Scale bar*, 10 μm.

5, *C* and *D*) that correlated well with that for adult mouse retina reported by Pochet *et al.* (45). Marked cellular staining was found in the outer and inner part of the inner nuclear layer (INL) as well as in some radial processes running through the INL. Cells in the ganglion cell layer (GCL) were also labeled, and punctate staining was observed in the inner plexiform layer (IPL), reminiscent of synaptic structures. There was only faint CaM immunoreactivity in structures related to photoreceptors, *i.e.* the ONL or the inner and outer segments.

In subsequent experiments, antibodies recognizing total CaMKII were used (Fig. 5, *E* and *F*). We found kinase expression within GCL and INL cell groups of the PN11 retina in a pattern generally compatible with previous reports in adult mouse retina (46). Total CaMKII staining was also observed in the outer retina, including in the photoreceptor segments (see Fig. 5, *E* and *F*, *insets*). Furthermore no staining differences were observed between rd1 and WT retinae in agreement with our lack of differential CaMKII protein detection on 2DE comparisons. However, alterations in enzyme activity may not necessarily reflect differences in its expression pattern. To address the question of differential CaMKII activation despite similar retinal expression patterns in the two genotypes, we used antibodies specifically recognizing CaMKII phosphorylated at Thr-286. Addition of a phosphate group at this amino acid occurs by autophosphorylation following stimulation of the enzyme by Ca^{2+} and CaM, thus activating the kinase (44). Thus, the phosphorylation of CaMKII at Thr-286 marks the active state of this kinase (see *e.g.* Ref. 47). Fig. 5, *G* and *H*, shows that staining with an anti-Thr-286 pCaMKII antibody produced similar immunoreactive patterns for rd1 and WT in IPL and outer plexiform layer as well as cytoplasmic staining in certain cells of the innermost INL and GCL. These results generally agree with those of Liu *et al.* (46) for the adult mouse retina, and both the IPL and outer plexiform layer staining would be compatible with the suggested presence and function for CaMKII in synapses (48). However, a higher optical resolution suggested a significant difference in pCaMKII staining in photoreceptors (not clearly resolved in Fig. 5, *G* and *H*) whereby fewer pCaMKII-positive OS were found for WT than rd1. The decreased number and the spacing suggested that pCaMKII-positive OS in WT could be allocated to cones. Consequently co-stainings with PNA were done to discriminate cone segments (49), and the analyses were extended to include sections of dark-adapted WT and rd1 retinae analyzed

by confocal microscopy. The resulting higher resolution revealed that the pattern of pCaMKII activity visualized by pCaMKII staining strictly correlates with that in phosducin blotting experiments of rd1 and WT retinae under light/dark conditions (see Fig. 4*C*). Again the phosphorylation states of CaMKII at Thr-286, indicating active kinase in rd1 rod photoreceptors in both light and dark phases, were equal to the WT hyperphosphorylation state in darkness (Fig. 6, *B–D*). WT light phase specimens showed a restricted number of positive structures at regularly spaced intervals in the photoreceptor segment layer co-labeled with PNA, suggesting that CaMKII in this situation was active only in cone segments, particularly at their very distal outer ends (Fig. 6*A*). Upon dark adaptation most, if not all, of the remaining photoreceptor segments were positive for activated CaMKII, including those not labeled by PNA, and also here staining was observed at the distal most aspects of the segments (Fig. 6*C*). The WT structures that were immunopositive for activated CaMKII in the dark greatly outnumbered the PNA co-labeled cones. Furthermore these stained structures were located closer to the retinal pigment epithelium face compared with PNA-co-labeled cones, clearly indicating the activation of CaMKII in rod outer segments (Fig. 6*C*). Together these findings suggested that CaMKII was active in WT rods solely in the dark. This situation was clearly different from that of the rd1 retina in which activated CaMKII was seen in both rods and cones of both light and dark phases (Fig. 6, *B* and *D*). The pCaMKII staining thus suggests that the calcium-dependent kinase CaMKII that could be responsible for phosducin hyperphosphorylation is constitutively activated in rd1 rods irrespective of the presence of light. It further suggests that, in yet unresolved molecular terms, the rd1 rods operate as rods do in a normal retina in the dark-adapted state. The above stainings were performed with the Thr-286 pCaMKII antibody from Cell Signaling Technology. Similar staining patterns could be produced with a different antibody (Thr-286 pCaMKII antibody, Promega; data not shown).

DISCUSSION

Five functionally unrelated proteins, COP9 subunit 8 (Csn8), 14-3-3 ζ, phosducin, β-adaptin, and guanylate kinase, were unambiguously differentially expressed in the rd1 retina at PN11. Of these, phosducin is generally regarded as confined to retinal photoreceptors (50), *i.e.* the cells directly affected in the rd1 model. There is at present no detailed information on the retinal expression of Csn8 and β-adaptin. Guanylate kinase and 14-3-3 ζ are also expressed in retinal cells other than photoreceptors.[3]

We found an up-regulation of Csn8, an evolutionary conserved integral part of the COP9 signalosome complex. COP9 is a regulatory component of the ubiquitin-proteasome pathway for regulated protein degradation (51, 52). Although the presence and function of COP9 in mouse retina have not been studied, its involvement in *Drosophila* eye development has been suggested (53). An association between Csn8 and retinal degeneration remains unknown. We also found the up-regulation of another protein in rd1, 14-3-3 ζ, which is abundantly expressed in retina (50, 54) and which has been demonstrated to bind phosducin upon phosphorylation by CaMKII (41).

Two proteins were down-regulated in rd1: β-adaptin and guanylate kinase. β-Adaptin is part of the AP2 coat assembly protein complex (55) involved in clathrin-mediated endocytosis of receptors (56, 57). In other tissues, β-adaptin combined with non-visual arrestins takes part in internalization of G protein-coupled receptors (GPCRs) (58) and thus contributes to GPCR desensitization and GPCR-induced signaling. However, the function of retinal β-adaptin is currently unknown, and although its down-regulation in the rd1 retina may indicate an impairment of a yet undefined interaction with rhodopsin, any relation to disease mechanisms must remain speculative. The other down-regulated protein identified in this study was guanylate kinase (GK), the first enzyme in the metabolic pathway that generates cGMP. GK phosphorylates 5′-GMP to GDP, which subsequently is phosphorylated by nucleoside-diphosphate kinase to GTP. GTP is then transformed into cGMP by calcium-dependent guanylate cyclase. Thus, GK is crucial for maintaining a certain cGMP level in the retina, *e.g.* photoreceptors (59), a prerequisite facilitating Ca^{2+} influx through the cGMP-gated cation channel. As mentioned, the rd1 mutation renders PDE6-β inactive, so GK down-regulation may reflect a feedback response from continually elevated cGMP levels.

Phosducin is exclusively expressed in photoreceptors, making this protein a particularly interesting candidate for further investigation especially because the detected regulation on 2DE analysis depended upon a post-translational modification of the protein. Phosducin is a *bona fide* retinal phosphoprotein (39, 41), and both our 2DE results and Western blot data were compatible with increased phosducin phosphorylation in the rd1 retina. Although phosphorylation of phosducin was thought to occur primarily by a cAMP-dependent protein kinase (PKA) and to lesser extent by GRK-2, phosphorylating phosducin at one position each (39, 40), recent results indicate that phosducin is additionally phosphorylated by CaMKII (41, 42). All seven phosducin spots detected here by 2DE were quantitatively different between rd1 and WT (Fig. 4*A*), indicating that although PKA (and GRK-2) may have been involved in altering one (or two) of the phosphorylation variants, other kinases, including calcium-dependent kinases, could also have contributed to the differential phosphorylation. The localization of activated CaMKII to the outer segment of the rd1 rod photoreceptors, where relevant interactions with phosducin are likely to occur, makes this kinase an attractive candidate for at least some of the

[3] P. A. R. Ekström, F. Paquet-Durand, and T. van Veen, unpublished observations.

altered phosducin phosphorylation.

In photoreceptors, phosducin binds to the β-γ subunits of transducin to facilitate their translocation from outer to inner segments (43). The binding requires a dephosphorylated state of phosducin, which in turn depends on the light status. In the dark, high photoreceptor Ca^{2+} levels (60) are accompanied by high phosducin phosphorylation, and with light adaptation phosducin becomes dephosphorylated as Ca^{2+} decreases (61, 62). Thus, in the light state dephosphorylated phosducin binds transducin β-γ with high efficiency and helps to move the latter to the inner segment of the photoreceptors (37, 38, 43). As a consequence, the outer segment signal flow from rhodopsin to cGMP-PDE utilizing transducin is dampened, and the sensitivity of light-adapted rods is therefore reduced (43).

For the WT situation, our studies of dark-adapted retinae demonstrated increased phosducin phosphorylation as well as CaMKII activation in rod photoreceptor segments when compared with the light phase. This corroborates the view that CaMKII participates in phosducin phosphorylation and that the latter is counteracted by light (41, 42). However, in the rd1 retina, the light-dependent regulation of CaMKII activation as well as phosducin phosphorylation was found to be impaired. There is consensus on increased Ca^{2+} levels in rd1 photoreceptors (7, 8, 13, 14), and high Ca^{2+} has likely contributed to the constitutive activation of CaMKII, which thus in turn could have contributed to the increased phosducin phosphorylation in rd1 independently of light conditions. However, it should be noted that an involvement of other Ca^{2+}-dependent kinases cannot be ruled out in this context.

Does increased phosducin phosphorylation by *e.g.* CaMKII promote or participate in rd1 photoreceptor degeneration, or is it solely consequential to events leading to photoreceptor death? It seems unlikely that continuous phosducin phosphorylation on its own drives rod degeneration as retinal damage should then be expected from light deprivation alone in WT mice. However, although experiments demonstrate the importance of light in the maturation of synaptic function in inner retina, no indications exist for light deprivation-induced degenerative processes in normal animals (63). It is noteworthy that CaMKII expression can be influenced by light exposure. Increased CaMKII mRNA and protein levels have been found in the retina of dark-reared PN12 rats (64), suggesting that elevated CaMKII in dark-reared animals phosphorylates the GluR1 subunit of the α-amino-3-hydroxy-5-methyl-4-isoxazolepropionic acid glutamate receptors and in consequence affects synaptic maturation as already demonstrated for CaMKII in brain (65, 66). Although total CaMKII protein levels were unchanged in our studies, the observed strong difference in rod phospho-CaMKII immunostaining between light- and dark-adapted WT PN11 retinae confirms a link between CaMKII activity and light/dark status. The disease-induced and constitutive CaMKII activation may therefore affect the normal synaptic development in the rd1 retina.

CaMKII activity requires a Ca^{2+}-binding protein (CaBP) like CaM for activation (44), but the presence of CaM in photoreceptors has been difficult to assess. Pochet *et al.* (45) reported lack of immunoreactivity in mouse photoreceptors, which fits well with the very weak CaM signal in ONL and inner and outer segments in this study. On the other hand, CaM was detected in feline and bovine OS by ultrastructural immunostaining and biochemical methods, respectively (67, 68). Furthermore using *in situ* hybridization, Kovacs and Gulya (69) observed low levels of CaM mRNA in the rat retina at the myoid (inner segment) portion of the photoreceptors where protein synthesis occurs (70). Other CaBPs may augment or even substitute for CaM function (71). Several of these are able to stimulate CaMKII (71), and at least one, CaBP4, is expressed by photoreceptors (72). The presence of CaBPs may therefore compensate for the relative paucity of CaM in photoreceptors.

Although CaMKII activity in light-adapted rd1 rods seems to resemble the dark-adapted WT state, the consequences of continually elevated CaMKII activity combined with constitutively raised Ca^{2+} levels are likely to create a distinct pathological phenotype in the rd1 mouse that differs from dark-adapted WT photoreceptors: Ca^{2+} modulation plays a crucial function in the development of the neuronal connectivity of the visual system and a regulatory role within mature photoreceptors in the conversion of the light signal received by photoreceptors into an electrical signal transmitted to the brain (73). Recent studies on guanylate cyclase (GC)-activating proteins (GCAP1–3), specific Ca^{2+}-sensitive regulators of retinal GC (for a review, see Ref. 74), have correlated these regulators and receptors for Ca^{2+} homeostasis to retinal pathological states, including genotypes associated with autosomal dominant cone-rod dystrophy (75, 76). Disease-linked GCAP1 mutations thus far identified are inherited in a dominant fashion, leading to augmented cGMP levels in the cytoplasm of rod and cone outer segments through increased GC activity, which results in constitutively higher intracellular Ca^{2+} levels in photoreceptors as the cGMP-gated channels remain open (77). As an upstream component of the same molecular network regulating intracellular Ca^{2+}, a stop mutation within the β subunit of PDE6 leads to retinal degeneration in the rd1 mouse. PDE6 removes cGMP, the product of guanylate cyclase activity, and can therefore be regarded as an indirect antagonist to GC. In the absence of functional PDE, photoreceptors suffer from a constitutive Ca^{2+} overload (7, 8). Consequently mutations in GCAP1 and PDE6 likely cause a similar pathological phenotype with respect to Ca^{2+} homeostasis that differs from the normal, dark-adapted state and that eventually leads to degeneration. Therefore and as suggested by for instance Frasson *et al.* (13) and Takano *et al.* (14), Ca^{2+} blockers may represent rational therapeutic agents for such forms of retinal degenerations. Within this context CaMKII activity as well as the differential phosphorylation of phosducin can be regarded as molecular markers of the de-

generating rd1 mouse retina. Future mechanistic and comparative studies in other models for genetically inherited retinal diseases are required to determine whether CaMKII activity represents a distinct surrogate marker for retinal degenerations or whether it is causatively linked to specific forms of this disease.

Acknowledgments—We thank Gitt Klefbohm for skillful help with animals and retinal samples, Stephanie Schöffmann for excellent assistance in proteomic techniques, and Dr. Ursula Olazabal for critical comments on the manuscript.

* This work was supported by grants from the Foundation Fighting Blindness, Stiftelsen för synskadade i före detta Malmöhus län, second ONCE international award for new technologies for the blind, the Crafoord Foundation, the Segerfalk Foundation, the Dutch Retina Foundation, Lund University Hospital funds, Kronprinsessan Margaretas Arbetsnämnd, European Union grants (PRO-AGE-RET: QLK6-CT-2001-00385, PRO-RET: QLK6-CT-2000-00569, RETNET: MRTN-CT-2003-504003, and EVI-GENORET: LSHG-CT-2005 512036), and grants from the German Federal Ministry of Education Research (BMBF-Functional Proteomics) (031U108A/03U208A). The costs of publication of this article were defrayed in part by the payment of page charges. This article must therefore be hereby marked "*advertisement*" in accordance with 18 U.S.C. Section 1734 solely to indicate this fact.

§ Both authors contributed equally to this work.

‖ To whom correspondence should be addressed. Tel.: 46-46-222-07-66; Fax: 46-46-222-07-74; E-mail: Per.Ekstrom@med.lu.se.

REFERENCES

1. Farber, D. B., Park, S., and Yamashita, C. (1988) Cyclic GMP-phosphodiesterase of rd retina: biosynthesis and content. *Exp. Eye. Res.* **46,** 363–374
2. Bowes, C., Li, T., Danciger, M., Baxter, L. C., Applebury, M. L., and Farber, D. B. (1990) Retinal degeneration in the rd mouse is caused by a defect in the β subunit of rod cGMP-phosphodiesterase. *Nature* **347,** 677–680
3. McLaughlin, M. E., Ehrhart, T. L., Berson, E. L., and Dryja, T. P. (1995) Mutation spectrum of the gene encoding the β subunit of rod phosphodiesterase among patients with autosomal recessive retinitis pigmentosa. *Proc. Natl. Acad. Sci. U. S. A.* **92,** 3249–3253
4. Farber, D. B., and Lolley, R. N. (1974) Cyclic guanosine monophosphate: elevation in degenerating photoreceptor cells of the C3H mouse retina. *Science* **186,** 449–451
5. Cobbs, W. H., and Pugh, E. N., Jr. (1985) Cyclic GMP can increase rod outer-segment light sensitive current 10-fold without delay of excitation. *Nature* **313,** 585–587
6. Fesenko, E. E., Kolesnikov, S. S., and Lyubarsky, A. L. (1985) Induction by cyclic GMP of a cationic conductance in plasma membrane of retinal rod outer segment. *Nature* **313,** 310–313
7. Fox, D. A., Poblenz, A. T., and He, L. (1999) Calcium overload triggers photoreceptor apoptotic cell death in chemical-induced and inherited retinal degenerations. *Ann. N. Y. Acad. Sci.* **893,** 282–285
8. Fox, D. A., Poblenz, A. T., He, L., Harris, J. B., and Medrano, C. J. (2003) Pharmacological strategies to block rod photoreceptor apoptosis caused by calcium overload: a mechanistic target-site approach to neuroprotection. *Eur. J. Ophthalmol.* **13,** Suppl. 3, S44–S56
9. He, L., Poblenz, A. T., Medrano, C. J., and Fox, D. A. (2000) Lead and calcium produce rod photoreceptor cell apoptosis by opening the mitochondrial permeability transition pore. *J. Biol. Chem.* **275,** 12175–12184
10. Chang, G. Q., Hao, Y., and Wong, F. (1993) Apoptosis: final common pathway of photoreceptor death in rd, rds, and rhodopsin mutant mice. *Neuron* **11,** 595–605
11. Lolley, R. N., Rong, H., and Craft, C. M. (1994) Linkage of photoreceptor degeneration by apoptosis with inherited defect in phototransduction. *Investig. Ophthalmol. Vis. Sci.* **35,** 358–362
12. Portera-Cailliau, C., Sung, C. H., Nathans, J., and Adler, R. (1994) Apoptotic photoreceptor cell death in mouse models of retinitis pigmentosa. *Proc. Natl. Acad. Sci. U. S. A.* **91,** 974–978
13. Frasson, M., Sahel, J. A., Fabre, M., Simonutti, M., Dreyfus, H., and Picaud, S. (1999) Retinitis pigmentosa: rod photoreceptor rescue by a calcium-channel blocker in the rd mouse. *Nat. Med.* **5,** 1183–1187
14. Takano, Y., Ohguro, H., Dezawa, M., Ishikawa, H., Yamazaki, H., Ohguro, I., Mamiya, K., Metoki, T., Ishikawa, F., and Nakazawa, M. (2004) Study of drug effects of calcium channel blockers on retinal degeneration of rd mouse. *Biochem. Biophys. Res. Commun.* **313,** 1015–1022
15. Jomary, C., Neal, M. J., and Jones, S. E. (2001) Characterization of cell death pathways in murine retinal neurodegeneration implicates cytochrome c release, caspase activation, and bid cleavage. *Mol. Cell. Neurosci.* **18,** 335–346
16. Kim, D. H., Kim, J.-A., Choi, J.-S., and Joo, C. K. (2002) Activation of caspase-3 during degeneration of the outer nuclear layer in the rd mouse. *Ophthalmic Res.* **34,** 150–157
17. Sharma, A. K., and Rohrer, B. (2004) Calcium-induced calpain mediates apoptosis via caspase-3 in a mouse photoreceptor cell line. *J. Biol. Chem.* **279,** 35564–35572
18. Doonan, F., Donovan, M., and Cotter, T. G. (2003) Caspase-independent photoreceptor apoptosis in mouse models of retinal degeneration. *J. Neurosci.* **23,** 5723–5731
19. Yoshizawa, K., Kiuchi, K., Nambu, H., Yang, J., Senzaki, H., Kiyozuka, Y., Shikata, N., and Tsubura, A. (2002) Caspase-3 inhibitor transiently delays inherited retinal degeneration in C3H mice carrying the rd gene. *Graefe's Arch. Clin. Exp. Ophthalmol.* **240,** 214–219
20. Zeiss, C. J., Neal, J., and Johnson, E. A. (2004) Caspase-3 in postnatal retinal development and degeneration. *Investig. Ophthalmol. Vis. Sci.* **45,** 964–970
21. Hopp, R. M., Ransom, N., Hilsenbeck, S. G., Papermaster, D. S., and Windle, J. J. (1998) Apoptosis in the murine rd1 retinal degeneration is predominantly p53-independent. *Mol. Vis.* **4,** 5–8
22. Hafezi, F., Abegg, M., Grimm, C., Wenzel, A., Stuermer, J., Farber, D. B., and Reme, C. E. (1998) Retinal degeneration in the rd mouse in the absence of c-fos. *Investig. Ophthalmol. Vis. Sci.* **38,** 2239–2244
23. Hafezi, F., Steinbach, J. P., Marti, A., Munz, K., Wang, Z. Q., Wagner, E. F., Aguzzi, A., and Reme, C. E. (1997) The absence of c-fos prevents light-induced apoptotic cell death of photoreceptors in retinal degeneration in vivo. *Nat. Med.* **3,** 346–349
24. Chen, J., Flannery, J. G., LaVail, M. M., Steinberg, R. H., Xu, J., and Simon, M. I. (1996) *bcl-2* overexpression reduces apoptotic photoreceptor cell death in three different retinal degenerations. *Proc. Natl. Acad. Sci. U. S. A.* **93,** 7042–7047
25. Dubois-Dauphin, M., Frankowski, H., Tsujimoto, Y., Huarte, J., and Martinou, J. C. (1994) Neonatal motoneurons overexpressing the bcl-2 protooncogene in transgenic mice are protected from axotomy-induced cell death. *Proc. Natl. Acad. Sci. U. S. A.* **91,** 3309–3313
26. Johnson, L. E., van Veen, T., and Ekström, P. A. (2005) Differential Akt activation in the photoreceptors of normal and rd1 mice. *Cell Tissue Res.* **320,** 213–222
27. Jones, S. E., Jomary, C., Grist, J., Stewart, H. J., and Neal, M. J. (2000) Identification by array screening of altered nm23-M2/PuF mRNA expression in mouse retinal degeneration. *Mol. Cell Biol. Res. Commun.* **4,** 20–25
28. Hackam, A. S., Strom, R., Liu, D., Qian, J., Wang, C., Otteson, D., Gunatilaka, T., Farkas, R. H., Chowers, I., Kageyama, M., Leveillard, T., Sahel, J. A., Campochiaro, P. A., Parmigiani, G., and Zack, D. J. (2004) Identification of gene expression changes associated with the progression of retinal degeneration in the rd1 mouse. *Investig. Ophthalmol. Vis. Sci.* **45,** 2929–2942
29. Rohrer, B., Pinto, F. R., Hulse, K. E., Lohr, H. R., Zhang, L., and Almeida, J. S. (2004) Multidestructive pathways triggered in photoreceptor cell death of the rd mouse as determined through gene expression profiling. *J. Biol. Chem.* **279,** 41903–41910
30. Cavusoglu, N., Thierse, D., Mohand-Said, S., Chalmel, F., Poch, O., Van Dorsselaer, A., Sahel, J. A., and Leveillard, T. (2003) Differential proteomic analysis of the mouse retina: the induction of crystallin proteins by retinal degeneration in the rd1 mouse. *Mol. Cell. Proteomics* **2,** 494–505
31. Hauck, S. M., Schöffmann, S., Deeg, C. A., Gloeckner, J. C., Swiatek-de Lange, M., and Ueffing, M. (2005) Proteomic analysis of porcine inter-

photoreceptor matrix. *Proteomics* **14,** 3623–3636
32. Blum, H., Beier, H., and Gross, H. J. (1987) Improved silver staining of plant proteins, RNA, and DNA in polyacrylamide gels. *Electrophoresis* **8,** 93–99
33. Gharahdaghi, F., Weinberg, C. R., Meagher, D. A., Imai, B. S., and Mische, S. M. (1999) Mass spectrometric identification of proteins from silver-stained polyacrylamide gel: a method for the removal of silver ions to enhance sensitivity. *Electrophoresis* **20,** 601–605
34. Perkins, D. N., Pappin, D. J., Creasy, D. M., and Cottrell, J. S. (1999) Probability-based protein identification by searching sequence databases using mass spectrometry data. *Electrophoresis* **20,** 3551–3567
35. Bowes, C., Danciger, M., Kozak, C. A., and Farber, D. B. (1989) Isolation of a candidate cDNA for the gene causing retinal degeneration in the rd mouse. *Proc. Natl. Acad. Sci. U. S. A.* **86,** 9722–9726
36. Farber, D. B., and Lolley, R. N. (1976) Enzymatic basis for cyclic GMP accumulation in degenerative photoreceptor cells of mouse retina. *J. Cyclic Nucleotide Res.* **2,** 139–148
37. Lee, R. H., Ting, T. D., Lieberman, B. S., Tobias, D. E., Lolley, R. N., and Ho, Y. K. (1992) Regulation of retinal cGMP cascade by phosducin in bovine rod photoreceptor cells. Interaction of phosducin and transducin. *J. Biol. Chem.* **267,** 25104–25112
38. Yoshida, T., Willardson, B. M., Wilkins, J. F., Jensen, G. J., Thornton, B. D., and Bitensky, M. W. (1994) The phosphorylation state of phosducin determines its ability to block transducin subunit interactions and inhibit transducin binding to activated rhodopsin. *J. Biol. Chem.* **269,** 24050–24057
39. Lee, R. H., Brown, B. M., and Lolley, R. N. (1990) Protein kinase A phosphorylates retinal phosducin on serine 73 *in situ*. *J. Biol. Chem.* **265,** 15860–15866
40. Ruiz-Gomez, A., Humrich, J., Murga, C., Quitterer, U., Lohse, M. J., and Mayor, F., Jr. (2000) Phosphorylation of phosducin and phosducin-like protein by G protein-coupled receptor kinase 2. *J. Biol. Chem.* **275,** 29724–29730
41. Thulin, C. D., Savage, J. R., McLaughlin, J. N., Truscott, S. M., Old, W. M., Ahn, N. G., Resing, K. A., Hamm, H. E., Bitensky, M. W., and Willardson, B. M. (2001) Modulation of the G protein regulator phosducin by Ca^{2+}/calmodulin-dependent protein kinase II phosphorylation and 14-3-3 protein binding. *J. Biol. Chem.* **276,** 23805–23815
42. Lee, B. Y., Thulin, C. D., and Willardson, B. M. (2004) Site-specific phosphorylation of phosducin in intact retina. Dynamics of phosphorylation and effects on G protein $\beta\gamma$ dimer binding. *J. Biol. Chem.* **279,** 54008–54017
43. Sokolov, M., Strissel, K. J., Leskov, I. B., Michaud, N. A., Govardovskii, V. I., and Arshavsky, V. Y. (2004) Phosducin facilitates light-driven transducin translocation in rod photoreceptors. Evidence from the phosducin knockout mouse. *J. Biol. Chem.* **279,** 19149–19156
44. Hudmon, A., and Schulman, H. (2002) Neuronal Ca^{2+}/calmodulin-dependent protein kinase II: the role of structure and autoregulation in cellular function. *Annu. Rev. Biochem.* **71,** 473–510
45. Pochet, R., Pasteels, B., Seto-Ohshima, A., Bastianelli, E., Kitajima, S., and Van Eldik, L. J. (1991) Calmodulin and calbindin localization in retina from six vertebrate species. *J. Comp. Neurol.* **314,** 750–762
46. Liu, L. O., Li, G., McCall, M. A., and Cooper, N. G. (2000) Photoreceptor regulated expression of Ca^{2+}/calmodulin-dependent protein kinase II in the mouse retina. *Brain Res. Mol. Brain Res.* **82,** 150–166
47. Means, A. R. (2000) Regulatory cascades involving calmodulin-dependent protein kinases. *Mol. Endocrinol.* **14,** 4–13
48. Kennedy, M. B. (1998) Signal transduction molecules at the glutamatergic postsynaptic membrane. *Brain Res. Brain Res. Rev.* **26,** 243–257
49. Fei, Y. (2003) Development of the cone photoreceptor mosaic in the mouse retina revealed by fluorescent cones in transgenic mice. *Mol. Vis.* **9,** 31–42
50. Nakano, K., Chen, J., Tarr, G. E., Yoshida, T., Flynn, J. M., and Bitensky, M. W. (2001) Rethinking the role of phosducin: light-regulated binding of phosducin to 14-3-3 in rod inner segments. *Proc. Natl. Acad. Sci. U. S. A.* **98,** 4693–4698
51. Lykke-Andersen, K., and Wei, N. (2003) Gene structure and embryonic expression of mouse COP9 signalosome subunit 8 (Csn8). *Gene* (*Amst.*) **321,** 65–72
52. Harari-Steinberg, O., and Chamovitz, D. A. (2004) The COP9 signalosome: mediating between kinase signaling and protein degradation. *Curr. Protein Pept. Sci.* **3,** 185–189
53. Suh, G. S., Poeck, B., Chouard, T., Oron, E., Segal, D., Chamovitz, D. A., and Zipursky, S. L. (2002) Drosophila JAB1/CSN5 acts in photoreceptor cells to induce glial cells. *Neuron* **33,** 35–46
54. Roseboom, P. H., Weller, J. L., Babila, T., Aitken, A., Sellers, L. A., Moffett, J. R., Namboodiri, M. A., and Klein, D. C. (1994) Cloning and characterization of the ϵ and ζ isoforms of the 14-3-3 proteins. *DNA Cell Biol.* **13,** 629–640
55. Ponnambalam, S., Robinson, M. S., Jackson, A. P., Peiperl, L., and Parham, P. (1990) Conservation and diversity in families of coated vesicle adaptins. *J. Biol. Chem.* **265,** 4814–4820
56. Robinson, M. S. (1994) The role of clathrin, adaptors and dynamin in endocytosis. *Curr. Opin. Cell Biol.* **4,** 538–544
57. Druck, T., Gu, Y., Prabhala, G., Cannizzaro, L. A., Park, S.-H., Huebner, K., and Keen, J. H. (1995) Chromosome localization of human genes for clathrin adaptor polypeptides AP2-β and AP50 and the clathrin-binding protein, VCP. *Genomics* **30,** 94–97
58. Santini, F., Gaidarov, I., and Keen, J. H. (2002) G protein-coupled receptor/arrestin3 modulation of the endocytic machinery. *J. Cell Biol.* **156,** 665–676
59. Gaidarov, I. O., Suslov, O. N., and Abdulaev, N. G. (1993) Enzymes of the cyclic GMP metabolism in bovine retina. I. Cloning and expression of the gene for guanylate kinase. *FEBS Lett.* **335,** 81–84
60. Gray-Keller, M. P., and Detwiler, P. B. (1994) The calcium feedback signal in the phototransduction cascade of vertebrate rods. *Neuron* **13,** 849–861
61. Brown, B. M., Carlson, B. L., Zhu, X., Lolley, R. N., and Craft, C. M. (2002) Light-driven translocation of the protein phosphatase 2A complex regulates light/dark dephosphorylation of phosducin and rhodopsin. *Biochemistry* **41,** 13526–13538
62. Lee, R. H., Brown, B. M., and Lolley, R. N. (1984) Light-induced dephosphorylation of a 33K protein in rod outer segments of rat retina. *Biochemistry* **23,** 1972–1977
63. Tian, N., and Copenhagen, D. R. (2001) Visual deprivation alters development of synaptic function in inner retina after eye opening. *Neuron* **32,** 439–449
64. Xue, J., Li, G., Laabich, A., and Cooper, N. G. (2001) Visual-mediated regulation of retinal CaMKII and its GluR1 substrate is age-dependent. *Mol. Brain Res.* **93,** 95–104
65. Benke, T. A., Luthi, A., Isaa, J. T., and Collinridge, G. L. (1998) Modulation of AMPA receptor unitary conductance by synaptic activity. *Nature* **393,** 793–797
66. Derkach, V., Barria, A., and Soderling, T. R. (1999) Ca^{2+}/calmodulin-kinase II enhances channel conductance of α-amino-3-hydroxy-5-methyl-4-isoxazolepropionate type glutamate receptors. *Proc. Natl. Acad. Sci. U. S. A.* **96,** 3269–3274
67. Wakakura, M., and Yamamoto, N. (1987) Immunological localization of calmodulin in feline rod outer segments. *Exp. Eye Res.* **44,** 451–458
68. Hsu, Y. T., and Molday, R. S. (1994) Interaction of calmodulin with the cyclic GMP-gated channel of rod photoreceptor cells. Modulation of activity, affinity purification, and localization. *J. Biol. Chem.* **269,** 29765–29770
69. Kovacs, B., and Gulya, K. (2003) Calmodulin gene expression in the neural retina of the adult rat. *Life Sci.* **73,** 3213–3224
70. Hargrave, P. A. (1986) Molecular dynamics of the rod cell, in *The Retina. A Model for Cell Biology Studies. Part I.* (Adler, R., and Farber, D., eds) pp. 207–237, Academic Press, New York
71. Haeseleer, F., Sokal, I., Verlinde, C. L., Erdjument-Bromage, H., Tempst, P., Pronin, A. N., Benovic, J. L., Fariss, R. N., and Palczewski, K. (2000) Five members of a novel Ca^{2+}-binding protein (CABP) subfamily with similarity to calmodulin. *J. Biol. Chem.* **275,** 1247–1260
72. Haeseleer, F., Imanishi, Y., Maeda, T., Possin, D. E., Maeda, A., Lee, A., Rieke, F., and Palczewski, K. (2004) Essential role of Ca^{2+}-binding protein 4, a Cav1.4 channel regulator, in photoreceptor synaptic function. *Nat. Neurosci.* **10,** 1079–1087
73. Haeseleer, F., Imanishi, Y., Sokal, I., Filipek, S., and Palczewski, K. (2002) Calcium-binding proteins: intracellular sensors from the calmodulin superfamily. *Biochem. Biophys. Res. Commun.* **290,** 615–623
74. Palczewski, K., Sokal, I., and Baehr, W. (2004) Guanylate cyclase-activating proteins: structure, function, and diversity. *Biochem. Biophys. Res. Commun.* **322,** 1123–1130
75. Nishiguchi, K. M., Sokal, I., Yang, L., Roychowdhury, N., Palczewski, K.,

Berson, E. L., Dryja, T. P., and Baehr, W. (2004) A novel mutation (I143NT) in guanylate cyclase-activating protein 1 (GCAP1) associated with autosomal dominant cone degeneration. *Investig. Ophthalmol. Vis. Sci.* **45,** 3863–3870

76. Sokal, I., Dupps, W. J., Grassi, M. A., Brown, J., Jr., Affatigato, L. M., Roychowdhury, N., Yang, L., Filipek, S., Palczewski, K., Stone, E. M., and Baehr, W. (2005) A novel GCAP1 missense mutation (L151F) in a large family with autosomal dominant cone-rod dystrophy (adCORD). *Investig. Ophthalmol. Vis. Sci.* **46,** 1124–1132
77. Olshevskaya, E. V., Calvert, P. D., Woodruff, M. L., Peshenko, I. V., Savchenko, A. B., Makino, C. L., Ho, Y. S., Fain, G. L., and Dizhoor, A. M. (2004) The Y99C mutation in guanylyl cyclase-activating protein 1 increases intracellular Ca^{2+} and causes photoreceptor degeneration in transgenic mice. *J. Neurosci.* **24,** 6078–6085